

Special Section on Transporters in Drug Disposition and Pharmacokinetic Prediction

Brain Distribution of a Novel MEK Inhibitor E6201: Implications in the Treatment of Melanoma Brain Metastases

Gautham Gampa, Minjee Kim, Nicholas Cook-Rostie, Janice K. Laramy, Jann N. Sarkaria, Linda Paradiso, Louis DePalatis, and William F. Elmquist

Brain Barriers Research Center, Department of Pharmaceutics, College of Pharmacy, University of Minnesota, Minneapolis, Minnesota (G.G., M.K., N.C.-R., J.K.L., W.F.E.); Radiation Oncology, Mayo Clinic, Rochester, Minnesota (J.N.S.); and Strategia Therapeutics Inc., Spring, Texas (L.P., L.D.)

Received October 26, 2017; accepted January 30, 2018

ABSTRACT

Clinically meaningful efficacy in the treatment of brain tumors, including melanoma brain metastases (MBM), requires selection of a potent inhibitor against a suitable target, and adequate drug distribution to target sites in the brain. Deregulated constitutive signaling of mitogen-activated protein kinase (MAPK) pathway has been frequently observed in melanoma, and mitogen-activated protein/extracellular signal-regulated kinase (MEK) has been identified to be an important target. E6201 is a potent synthetic small-molecule MEK inhibitor. The purpose of this study was to evaluate brain distribution of E6201, and examine the impact of active efflux transport at the blood-brain barrier on the central nervous system (CNS) exposure of E6201. In vitro studies utilizing transfected Madin-Darby canine kidney II (MDCKII) cells indicate that E6201 is not a substrate of P-glycoprotein (P-gp) and breast cancer

resistance protein (Bcrp). In vivo studies also suggest a minimal involvement of P-gp and Bcrp in E6201's brain distribution. The total concentrations in brain were higher than in plasma, resulting in a brain-to-plasma AUC ratio (K_p) of 2.66 in wild-type mice. The brain distribution was modestly enhanced in *Mdr1a/b*^{-/-}, *Bcrp1*^{-/-}, and *Mdr1a/b*^{-/-}*Bcrp1*^{-/-} knockout mice. The nonspecific binding of E6201 was higher in brain compared with plasma. However, free-drug concentrations in brain following 40 mg/kg intravenous dose reach levels that exceed reported in vitro half-maximal inhibitory concentration (IC₅₀) values, suggesting that E6201 may be efficacious in inhibiting MEK-driven brain tumors. The brain distribution characteristics of E6201 make it an attractive targeted agent for clinical testing in MBM, glioblastoma, and other CNS tumors that may be effectively targeted with inhibition of MEK signaling.

Introduction

Aberrant signaling of the mitogen-activated protein kinase (MAPK) pathway has been observed in about 80% of melanomas and various other types of cancers (Davies et al., 2002). The discovery of activating mutations in the BRAF oncogene, observed in about 50% of melanoma patients, has led to significant advances in therapeutic options for metastatic melanoma (Hocker and Tsao, 2007; Samatar and Poulikakos, 2014). Melanoma patients treated with the newly developed molecularly targeted therapies, e.g., mutant BRAF inhibitors such as vemurafenib and dabrafenib, mitogen-activated protein/extracellular signal-regulated kinase (MEK) inhibitors such as trametinib and

cobimetinib, have shown improvements in overall survival (OS) (Falchook et al., 2012; Long et al., 2012; Cohen et al., 2016; Margolin, 2016; Spagnolo et al., 2016). However, initial responses are often followed by eventual relapse associated with resistance, occurring via mechanisms that cause subsequent hyperactivated downstream MEK signaling (Lito et al., 2013; Samatar and Poulikakos, 2014). In patients with activating BRAF mutations, treatment with BRAF and MEK-inhibitor combination showed improved responses compared with single-agent therapy and is an important treatment strategy (Flaherty et al., 2012; Larkin et al., 2014; Ribas et al., 2014).

The burden of metastatic melanoma is projected to exceed 87,000 new cases and 9700 deaths in the United States in 2017 (Siegel et al., 2017). Approximately 70% of patients with metastatic melanoma will develop brain metastases in their lifetime, and after a diagnosis of metastatic spread to the brain, the median OS is less than 6 months (Gupta et al., 1997; Raizer et al., 2008; Sloan et al., 2009; Damsky et al., 2014). Focal therapies with surgical resection and/or radiosurgery can effectively control an individual metastasis, but the risk of developing subsequent brain metastases elsewhere in the brain

This work was supported by the National Institutes of Health [Grants RO1-NS077921 RO1-NS073610 and U54-CA210180] and Strategia Therapeutics Inc. Gautham Gampa was supported by the Ronald J. Sawchuk Fellowship in Pharmacokinetics.

<https://doi.org/10.1124/dmd.117.079194>.

ABBREVIATIONS: AUC, area under the curve; BBB, blood-brain barrier; Bcrp, breast cancer resistance protein; CNS, central nervous system; DA, distribution advantage; fu, free (unbound) fraction; FVB, Friend leukemia virus strain B; HBD, hydrogen-bond donor; IC₅₀, half-maximal inhibitory concentration; K_p, brain-to-plasma ratio; K_{p,uu}, unbound (free) brain-to-plasma ratio/unbound partition coefficient; LC-MS/MS, liquid chromatography-tandem mass spectroscopy; MAPK, mitogen-activated protein kinase; MBM, melanoma brain metastases; MDCKII, Madin-Darby canine kidney II; MEK, mitogen-activated protein/extracellular signal-regulated kinase; OS, overall survival; PBS, phosphate-buffered saline; P-gp, P-glycoprotein; RED, rapid equilibrium dialysis; WT, wild type.

exceeds 50%, which suggests that integrating these procedures with effective targeted therapies may provide significant clinical benefit (Fife et al., 2004). The successful treatment of brain tumors will need targeted therapies that are: 1) potent against its target, 2) capable of penetrating an intact blood-brain barrier (BBB) replete with efflux transporters (Osswald et al., 2016), and 3) capable of reaching the protected tumor cells that are not clinically detectable upon contrast-enhancing magnetic resonance imaging (Murrell et al., 2015). Many small-molecule molecularly-targeted therapies have limited ability to permeate an intact BBB, which in turn can limit their efficacy against brain tumors (Agarwal et al., 2011; Gampa et al., 2016, 2017). Although the BBB at the core of larger brain tumors has been observed to be compromised, certain regions of such tumors and micrometastases can have a relatively intact BBB (Essig et al., 2006; Murrell et al., 2015; Osswald et al., 2016). Active drug efflux, mainly by P-glycoprotein (P-gp) and breast cancer resistance protein (Bcrp), is a key mechanism responsible for limiting the entry of various xenobiotics into the brain especially at sites with an intact BBB, including molecularly targeted therapies approved for melanoma, such as vemurafenib, dabrafenib, trametinib, and cobimetinib (Mittapalli et al., 2012, 2013; Choo et al., 2014; Vaidhyanathan et al., 2014). As a consequence, drug delivery to tumor cells residing behind an intact BBB can be severely restricted, causing the establishment of a pharmacological sanctuary. There is a critical need to overcome issues related to brain drug delivery, and develop effective targeted therapies that can penetrate an intact BBB and reach the target sites on the tumor cells in the brain (Heffron, 2016).

E6201 (Fig. 1) is a natural product-inspired synthetic nonallosteric kinase inhibitor that inhibits both MEK1 and FLT3 (Ikemori-Kawada et al., 2012). E6201 is an ATP-competitive MEK inhibitor, in contrast to clinically approved drugs like trametinib and cobimetinib that are allosteric MEK inhibitors (Narita et al., 2014). The binding affinity of E6201 has been shown to be identical for both the active and inactive forms of MEK1 (Goto et al., 2009). The reported in vitro half-maximal inhibitory concentration (IC_{50}) for E6201 against multiple melanoma cell lines (particularly BRAF mutant lines) was less than 100 nmol/l, indicating that E6201 exhibits potent activity against melanoma cells (Byron et al., 2012; Narita et al., 2014).

Given that melanoma has a high propensity to metastasize to the CNS, and inhibition of MEK has been recognized to be an important strategy in treating metastatic melanoma, testing the ability of E6201 to permeate an intact BBB would be essential. The purpose of this study was to determine the brain distribution of E6201 and evaluate the role of major BBB efflux proteins, P-gp and/or Bcrp, in limiting the brain delivery of E6201, using mouse models. Such information can be valuable in evaluating the utility of this agent as an effective therapy for patients with melanoma brain metastases (MBM), and can inform future clinical trials. A brain-penetrant MEK inhibitor would be particularly useful in patients with MBM, and as such would hold great promise for the treatment of metastatic melanoma.

Materials and Methods

Chemicals

E6201 [(3S,4R,5Z,8S,9S,11E)-14-(ethylamino)-8,9,16-trihydroxy-3,4-dimethyl-3,4,9,10-tetrahydro-1H-2-benzoxacyclotetradecine-1,7(8H)-dione)] and ER807551

were kindly provided by Strategia Therapeutics Inc. (Houston, TX). [3H]-Vinblastine was purchased from Moravsek Biochemicals (La Brea, CA). [3H]-Prazosin was purchased from PerkinElmer Life and Analytical Sciences (Waltham, MA). Ko143 [(3S,6S,12aS)-1,2,3,4,6,7,12,12a-octahydro-9-methoxy-6-(2-methylpropyl)-1,4-dioxopyrazino(1',2':1,6) pyrido(3,4-b)indole-3-propanoic acid 1,1-dimethylethyl ester] was purchased from Tocris Bioscience (Ellisville, MO). Zosuquidar [LY335979, (R)-4-([1aR, 6R,10bS]-1,2-difluoro-1,1a,6,10b-tetrahydrodibenzo[a,e] cyclopropa [c]cycloheptan-6-yl)-[5-quinoloyloxy] methyl-1-piperazine ethanol, trihydrochloride] was provided by Eli Lilly and Co. (Indianapolis, IN). All other chemicals used were of high-performance-liquid-chromatography or reagent grade and were obtained from Sigma-Aldrich (St. Louis, MO).

In Vitro Accumulation Studies

Polarized Madin-Darby canine kidney II (MDCKII) cells were used for performing in vitro accumulation studies. MDCKII wild-type and Bcrp1-transfected (MDCKII-Bcrp1) cell lines were a kind gift from Dr. Alfred Schinkel (The Netherlands Cancer Institute). MDCKII wild-type and gene encoding the human P-glycoprotein (MDR1)-transfected (MDCKII-MDR1) cell lines were kindly provided by Dr. Piet Borst (The Netherlands Cancer Institute). Cells were cultured in Dulbecco's modified Eagle's medium supplemented with 10% (v/v) fetal bovine serum and antibiotics (penicillin, 100 IU/ml; streptomycin, 100 mg/ml; and amphotericin B, 250 ng/ml). Cells were grown in 25-ml tissue culture-treated flasks before seeding for the intracellular accumulation experiments and were maintained at 37°C in a humidified incubator with 5% carbon dioxide.

The intracellular accumulation of E6201 was performed in 12-well polystyrene plates (Corning Glassworks, Corning, NY). In brief, cells were seeded at a density of 2×10^5 cells and grown until ~80% confluent. On the day of experiment, the culture media was aspirated and the cells were washed two times with warm cell assay buffer (122 mM NaCl, 25 mM $NaHCO_3$, 10 mM glucose, 10 mM HEPES, 3 mM KCl, 2.5 mM $MgSO_4$, 1.8 mM $CaCl_2$, and 0.4 mM K_2HPO_4). The cells were then preincubated with cell assay buffer for 30 minutes, after which the buffer was aspirated and the experiment was initiated by adding 1 ml assay buffer containing 5 μM E6201 into each well with further incubation for 60 minutes in an orbital shaker (Shel Lab; Sheldon Manufacturing Co., Cornelius, OR) maintained at 37°C and 60 rpm. At the end of a 60-minute incubation, the experiment was ended by aspirating the E6201 solution followed by washing twice with ice-cold phosphate-buffered saline (PBS). The cell lysis was accomplished by adding 500 μl of 1% Triton-X100 to each well. When the inhibitor was used, it was included in both preincubation and accumulation steps. The concentration of E6201 in solubilized cell fractions was analyzed using liquid chromatography-tandem mass spectrometry (LC-MS/MS) as described later, and was normalized to the protein content (BCA assay).

In Vitro Binding Assays for Determination of Free (Unbound) Fraction of E6201 and Trametinib

The free fractions of E6201 in plasma and brain were determined by performing rapid equilibrium dialysis (RED) experiments per the protocol described by the manufacturer, with some modifications suggested in the literature (Kalvass and Maurer, 2002; Friden et al., 2007). RED base plate (Thermo Fisher Scientific, Waltham, MA), and single-use RED inserts (Thermo Fisher Scientific) with 8-kDa molecular weight cut off were used for these experiments. Briefly, fresh plasma and brain homogenates (prepared in three volumes of PBS, w/v) isolated from wild-type Friend leukemia virus strain

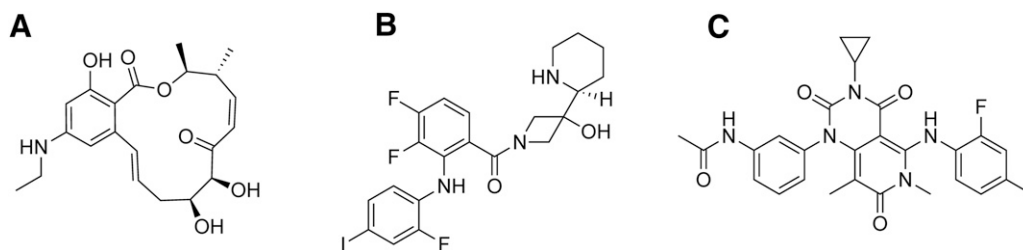


Fig. 1. Chemical structure of (A) E6201, (B) cobimetinib, and (C) trametinib.

B (FVB) mice were used. E6201 stock in dimethyl sulfoxide (DMSO) (1 mg/ml) was spiked in plasma and brain homogenate to obtain final concentrations of 10 μ M (DMSO <1% of final volume). Three-hundred microliters of 10 μ M E6201-spiked plasma/brain homogenate was placed in the sample chamber (donor), and 500 μ l of phosphate-buffered saline (1 \times PBS at pH 7.4; 100 mM sodium phosphate and 150 mM sodium chloride) was placed in buffer chamber (receiver) of the RED inserts, in triplicates. The inserts were placed in a base plate, the assembly covered with sealing tape, and incubated on an orbital shaker (Shel Lab) at 37°C and 300 rpm for 4 hours (preliminary studies show that equilibrium is achieved by 4 hours). After dialysis, 150 μ l of both plasma/brain homogenate and buffer were collected and the concentrations of E6201 were determined by liquid chromatography–tandem mass spectroscopy (LC-MS/MS). The brain-to-plasma ratio (Kp) for trametinib has been previously reported in literature, but the free (unbound) fraction (fu) was not available. So, RED experiments were performed to determine the free fractions of trametinib in plasma and brain, as described for E6201. The experiments were performed with a concentration of 2 μ M trametinib in both plasma and brain matrices.

In Vivo Studies

Animals. Friend leukemia virus strain B wild-type (WT), *Mdr1a/b*^{-/-} (P-gp knockout), *Bcrp1*^{-/-} (Bcrp knockout), and *Mdr1a/b*^{-/-} *Bcrp1*^{-/-} (triple knockout) mice of either sex (balanced) were used for all the in vivo studies (Taconic Farms, Germantown, NY). All mice used were 8–16 week-old adults, approximately 18–35 g, at the time of the experiments. Mice were maintained in a 12-hour light/dark cycle with unlimited access to food and water. All studies carried out were in agreement with the guidelines set by Principles of Laboratory Animal Care (National Institutes of Health, Bethesda, MD), and approved by Institutional Animal Care and Use Committee (IACUC) at University of Minnesota.

Plasma and Brain Pharmacokinetics of E6201 after Intravenous, Intraperitoneal, and Oral Administration. All dosing solutions were freshly prepared on the day of the experiment. E6201 dosing formulation was prepared by reconstituting lyophilized powder in single-use vials (received from Strategia Therapeutics Inc.), containing 60 mg E6201 and 3 g Captisol, with 8.5 ml of sterile water for injection.

In the first set of studies, an intravenous bolus dose of 40 mg/kg E6201 (a dose previously used in efficacy studies, E6201 investigators brochure; personal communication, Strategia Therapeutics) was administered to FVB wild-type, *Mdr1a/b*^{-/-}, *Bcrp1*^{-/-}, and *Mdr1a/b*^{-/-} *Bcrp1*^{-/-} knockout mice via tail vein. Blood and brain samples were harvested at 0.083, 0.25, 0.5, 1, 2, 4, and 6 hours postdose in a serial sacrifice (destructive sampling) design ($n = 5$ at each time point). At the desired sample-collection time point, the animals were euthanized using a carbon dioxide chamber. Blood was collected by cardiac puncture in heparinized tubes. The whole brain was removed from the skull and washed with ice-cold distilled water, and superficial meninges were removed by blotting with tissue paper. Plasma was separated by centrifugation of whole blood at 3500 rpm and 4°C for 15 minutes. Both plasma and brain samples were stored at -80°C until further analysis for E6201 concentrations by LC-MS/MS. Brain concentrations were corrected for residual drug in brain vasculature assuming a vascular volume of 1.4% in mouse brain (Dai et al., 2003).

In the second set of in vivo studies, 40 mg/kg E6201 was administered to FVB wild-type and *Mdr1a/b*^{-/-} *Bcrp1*^{-/-} knockout mice via intraperitoneal (i.p.) route. Blood and brain samples were harvested at 0.25, 0.5, 1, 2, 4, and 6 hours postdose in a serial sacrifice design ($n = 4$ at each time point) as described for intravenous studies.

In the third study, 40 mg/kg E6201 was administered to FVB wild-type mice via oral gavage (PO). Blood and brain samples were harvested at 0.25, 0.5, 1, 2, 4, and 6 hours postdose in a serial sacrifice design ($n = 4$ at each time point) as described for intravenous studies.

LC-MS/MS Analysis

The concentrations of E6201 in all samples from in vitro and in vivo studies were determined using a specific and sensitive LC-MS/MS assay. E6201 and samples/solutions containing E6201 were protected from light in all experiments to avoid drug degradation. Brain samples were homogenized using a mechanical homogenizer (PowerGen 125; Thermo Fisher Scientific) following the addition of three volumes of 5% bovine serum albumin to obtain uniform homogenates. For

analysis of unknowns, an aliquot of sample (cell lysate, cell assay buffer, PBS, plasma, or brain homogenate) was spiked with 50 ng of ER807551 as an internal standard and liquid-liquid extraction was performed by addition of 5–10 volumes of ethyl acetate, followed by vigorous shaking for 5 minutes and centrifugation at 7500 rpm and 4°C for 5 minutes. The organic layer was separated and transferred to microcentrifuge tubes, and dried under nitrogen gas. The dried powder was reconstituted in 100 μ l of mobile phase and transferred into high-performance liquid-chromatography glass vials with microinserts. Chromatographic analysis was performed using an AQUITY UPLC system (Waters, Milford, MA). The chromatographic separation was achieved by injection of 7.5- μ l sample onto a C18 YMC-ODS-AM (3- μ m particle size, 2.0 mm i.d. \times 23 mm length; YMC America, Allentown, PA) column. A gradient method was employed with mobile phase consisting of 0.1% formic acid in water as the aqueous component (A) and 0.1% formic acid in methanol as the organic component (B). The gradient was as follows: started with 35% B at 0 minutes, increased to 100% B by 0.5 minutes, and maintained at 100% B up to 3.2 minutes, decreased to 35% B by 3.5 minutes and maintained at 35% B up to 7 minutes. The mobile phase was delivered at a constant flow rate of 0.3 ml/min.

The column effluent was monitored using a Micromass Quattro Ultima mass spectrometer (Waters). The instrument was equipped with an electrospray interface, and controlled by the MassLynx (Version 4.1; Waters) data system. The samples were analyzed using an electrospray probe in the positive-ionization mode operating at a spray voltage of 2.5 kV for both E6201 and ER807551. Samples were introduced into the interface through a heated nebulized probe, in which the source temperature and desolvation temperature were set at 100 and 400°C, respectively. The mass spectrometer was programmed to allow the [MH]⁺ ions of E6201 and ER807551 at m/z ratios of 390.08 and 450.08, respectively, to pass through the first quadrupole (Q1) and into the collision cell (Q2). The collision energy was set at 20 and 25 V for E6201 and ER807551, respectively. The daughter ions for E6201 (m/z 232) and ER807551 (m/z 273.96) were monitored through the third quadrupole (Q3). The retention times for E6201 and ER807551 were 1.11 and 1.12 minutes, respectively. The runtime was 7 minutes.

Pharmacokinetic Analysis and Calculations

Pharmacokinetic parameters from the concentration-time profiles in plasma and brain were obtained by noncompartmental analysis (NCA) performed using Phoenix WinNonlin version 6.4 (Certara USA, Inc., Princeton, NJ). The area under the curves (AUC) for plasma (AUC_{plasma}) and brain (AUC_{brain}) were calculated using the linear trapezoidal method. The S.E. around the means of AUC and maximum drug concentration, C_{max}, were estimated using the sparse sampling module in WinNonlin (Nedelman and Jia, 1998).

Free (unbound) fractions (fu) in plasma and brain homogenate were calculated as the ratio of buffer-to-matrix concentrations of E6201 (Kalvass and Maurer, 2002).

$$fu, \text{ diluted} = \frac{\text{E6201 concentration in buffer(receiver)}}{\text{E6201 concentration in matrix(donor)}} \quad (1)$$

The fraction unbound for brain was determined from the measured fraction unbound in diluted brain homogenate (fu, diluted), using the following equation (Kalvass and Maurer, 2002).

$$fu, \text{ brain} = \frac{1/D}{(1/fu, \text{ diluted} - 1) + 1/D} \quad (2)$$

where D (equal to 4) represents the dilution factor, accounting for the diluted brain homogenate.

The recovery was estimated using the equation,

$$\text{Recovery}(\%) = \frac{(\text{donor mass} + \text{receiver mass}) \text{ after dialysis}}{\text{donor mass, before dialysis}} \times 100 \quad (3)$$

The brain-to-plasma ratio (Kp) was calculated as the ratio of AUC_{brain} to AUC_{plasma}.

$$Kp = \frac{AUC_{\text{brain}}}{AUC_{\text{plasma}}} \quad (4)$$

A comparison of relative drug exposure in the brain between wild-type and knockout (*Mdr1a/b*^{-/-}, *Bcrp1*^{-/-}, and *Mdr1a/b*^{-/-} *Bcrp1*^{-/-}) mice was made using the distribution advantage (DA).

$$DA = \frac{Kp, \text{knockout}}{Kp, \text{wild type}} \quad (5)$$

The unbound partition coefficient (Kp, uu) was calculated for the four genotypes using the equation,

$$Kp, uu = \frac{AUC_{\text{brain}} \times fu, \text{brain}}{AUC_{\text{plasma}} \times fu, \text{plasma}} \quad (6)$$

Statistical Analysis

GraphPad Prism version 6.04 (GraphPad, La Jolla, CA) software was used for the statistical analysis. The sample sizes used were based on previous work and were determined based on approximately 80% power to detect 50% difference between groups. Data from all experiments are represented as mean \pm S.D. or mean \pm S.E.M. unless otherwise indicated. Comparisons between two groups were made using an unpaired *t* test. Comparisons between multiple groups were made using one-way analysis of variance, followed by Bonferroni's multiple comparison test. A significance level of $P < 0.05$ was used for all statistical analysis.

Results

In Vitro Accumulation of E6201 in MDCKII-Bcrp1 and MDCKII-MDR1 Cells. The intracellular accumulation of E6201 in MDCKII wild-type, Bcrp1-transfected, and MDR1-transfected cell lines is summarized in Fig. 2. [³H]-Prazosin and [³H]-vinblastine were used as positive controls for Bcrp1 and MDR1, respectively. As expected, the cellular accumulation of [³H]-prazosin was significantly lower compared with wild-type controls (WT: 100% \pm 29%; Bcrp1: 25% \pm 5%; $P < 0.05$). Likewise, the cellular accumulation of [³H]-vinblastine was also significantly lower compared with wild-type controls (WT: 100% \pm 31%; MDR1: 7% \pm 1%; $P < 0.01$). These results validate the significant elevation of efflux transporter activity in the relevant transfected cell lines. In the same experiment, incubation with 5 μ M E6201 showed that the accumulation of E6201 was not significantly different in Bcrp1 cells (Bcrp1: 107% \pm 29%; WT: 100% \pm 29%), and in MDR1 cells (MDR1: 89% \pm 16%; WT: 100% \pm 9%) compared with

corresponding wild-type controls. The addition of 0.2 μ M Ko143, a specific Bcrp1 inhibitor, to the Bcrp1 cells and 1 μ M LY335979, a specific MDR1 inhibitor, to MDR1 cells did not lead to significant differences in intracellular accumulation compared with transfected cells without inhibitor. These data indicate that E6201 is not a substrate for either P-gp or Bcrp1.

Determination of Free (Unbound) Fraction of E6201 and Trametinib. In vitro rapid equilibrium dialysis was used for the determination of free fraction (eqs. 1 and 2) in plasma and brain. The free fraction (*fu*) for E6201 in plasma was determined to be 2.63% \pm 0.18%, and the mass balance recovery of the experiment was 94.04% \pm 3.32% (Table 1). The *fu* for E6201 in brain was found to be 0.14% \pm 0.02%, and the mass balance recovery was 113.20% \pm 9.50% (Table 1). The *fu* for trametinib in plasma was found to be 0.21% \pm 0.03%, and the mass balance recovery of the experiment was 99.9% \pm 8.42% (Table 1). The *fu* for trametinib in brain was determined to be 0.21% \pm 0.02%, and the mass balance recovery was 106.56% \pm 2.35% (Table 1). The estimated *fu* values were used for the determination of unbound partition coefficient, Kp, uu .

Plasma and Brain Pharmacokinetics following Intravenous, Intraperitoneal, and Oral E6201 Administration. The pharmacokinetic parameters for E6201 were determined in FVB wild-type and transporter-deficient (knockout) mice following various routes of E6201 administration. The brain and plasma concentration-time profiles and brain-to-plasma ratio profiles in FVB wild-type, *Mdr1a/b*^{-/-}, *Bcrp1*^{-/-}, and *Mdr1a/b*^{-/-} *Bcrp1*^{-/-} mice following a single i.v. bolus dose of 40 mg/kg E6201 are shown in Fig. 3. The total plasma E6201 concentrations (Fig. 3A) were similar between four genotypes at any given time point. The total brain E6201 concentrations (Fig. 3B) at the indicated time points were higher than the total plasma concentrations in all the four genotypes. Table 2 summarizes the estimated pharmacokinetic parameters in the four genotypes of mice studied. There were no statistically significant differences between the wild-type plasma AUC and any of the transporter knockout plasma AUCs. The estimated AUCs in the brain for *Mdr1a/b*^{-/-}, *Bcrp1*^{-/-}, and *Mdr1a/b*^{-/-} *Bcrp1*^{-/-} mice were significantly higher compared with the AUC in wild-type mice ($P < 0.05$). The observed systemic clearance and volume of distribution were similar in the wild-type and knockout mice. The brain-to-plasma AUC ratios (Kp , eq. 4) in the wild-type, *Mdr1a/b*^{-/-}, *Bcrp1*^{-/-}, and *Mdr1a/b*^{-/-} *Bcrp1*^{-/-} mice were 2.66, 4.37, 3.72, and 5.40,

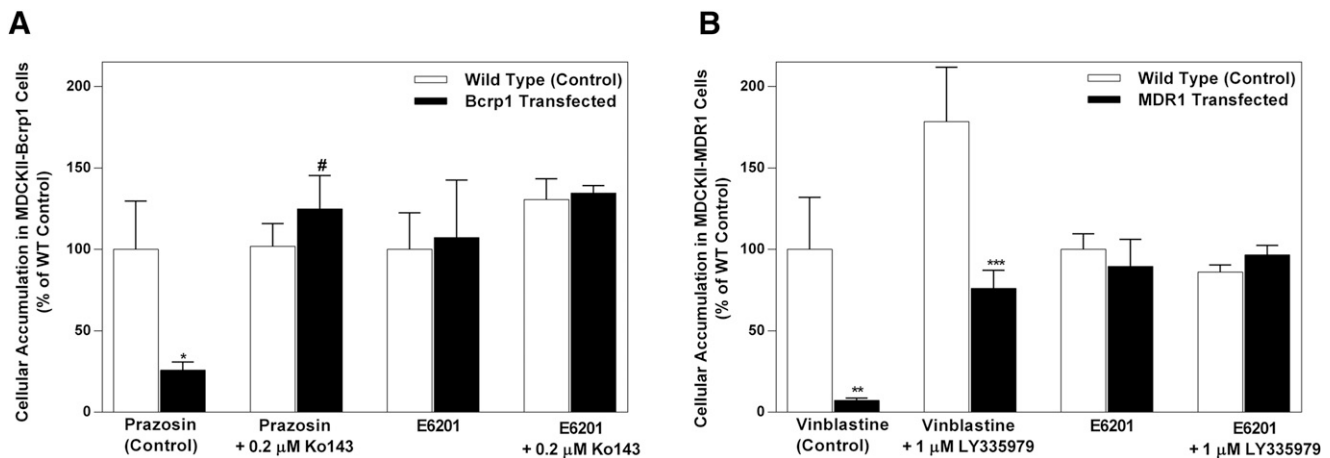


Fig. 2. In vitro intracellular accumulation of E6201. (A) The accumulation of prazosin (Bcrp probe substrate; positive control) and E6201 in MDCKII wild-type and Bcrp1-transfected cell lines with and without Bcrp inhibitor Ko143 (0.2 μ M). (B) The accumulation of E6201 and vinblastine (probe substrate for P-gp; positive control) in wild-type and MDR1-transfected cells with and without P-gp inhibitor LY335979 (1 μ M). Data represent the mean \pm S.D.; $n = 3$ for all data points. * $P < 0.05$ compared with respective wild-type controls; # $P < 0.01$ compared with the untreated transfected cell line; ** $P < 0.01$ compared with respective wild-type controls; *** $P < 0.001$ compared with the untreated transfected cell line.

TABLE 1

Free fraction for E6201 and trametinib in plasma and brain, determined by in vitro rapid equilibrium dialysis experiments

Data represent the mean \pm S.D. (n = 3).

Inhibitor	Matrix	fu	fu (%)	Recovery (%)	fu _{brain} /fu _{plasma}
E6201	Plasma	0.026 \pm 0.002	2.63 \pm 0.18	94.04 \pm 3.32	0.054
	Brain	0.0014 \pm 0.0002	0.14 \pm 0.02	113.20 \pm 9.49	—
Trametinib	Plasma	0.0021 \pm 0.0003	0.21 \pm 0.03	99.90 \pm 8.42	1
	Brain	0.0021 \pm 0.0002	0.21 \pm 0.02	106.56 \pm 2.35	—

respectively. A comparison of relative drug exposure in the brain between wild-type and knockout (*Mdr1a/b*^{-/-}, *Bcrp1*^{-/-}, and *Mdr1a/b*^{-/-} *Bcrp1*^{-/-}) mice was made using the DA, which is defined as the Kp in knockout mice normalized by the Kp in wild-type mice (eq. 5). The DA in *Mdr1a/b*^{-/-}, *Bcrp1*^{-/-}, and *Mdr1a/b*^{-/-} *Bcrp1*^{-/-} mice were 1.64, 1.39, and 2.03, suggesting minimal involvement of P-gp and Bcrp in limiting the brain distribution of E6201. The extent of distribution of free drug is represented by term “Kp,uu” and can be defined as the ratio of the unbound drug exposure in the brain over the unbound drug exposure in plasma (eq. 6). The Kp,uu in the wild-type, *Mdr1a/b*^{-/-}, *Bcrp1*^{-/-}, and *Mdr1a/b*^{-/-} *Bcrp1*^{-/-} mice were 0.14, 0.24, 0.20, and 0.29, respectively.

The concentration-time profiles and brain-to-plasma ratio profiles in FVB wild-type and *Mdr1a/b*^{-/-} *Bcrp1*^{-/-} mice following a single intraperitoneal dose of 40 mg/kg E6201 are shown in Fig. 4. The estimated pharmacokinetic parameters are summarized in Table 3. There was no statistically significant difference between the wild-type plasma AUC and *Mdr1a/b*^{-/-} *Bcrp1*^{-/-} plasma AUC. The AUC in the brain for *Mdr1a/b*^{-/-} *Bcrp1*^{-/-} mice was significantly higher compared with the AUC in wild-type mice ($P < 0.05$). The Kp value in wild-type and *Mdr1a/b*^{-/-} *Bcrp1*^{-/-} mice were 2.2 and 3.83, respectively. The

Kp,uu values in wild-type and *Mdr1a/b*^{-/-} *Bcrp1*^{-/-} mice were 0.12 and 0.21, respectively. The absolute bioavailability (F) following intraperitoneal administration was found to be 0.95.

The concentration-time profiles and brain-to-plasma ratio profile in FVB wild-type mice following single oral dose of 40 mg/kg E6201 are shown in Fig. 5. The estimated pharmacokinetic parameters are summarized in Table 4. The Kp and Kp,uu were found to be 2.35 and 0.13, respectively. The absolute bioavailability following oral administration was 0.39.

Discussion

The approved small-molecule targeted therapies for melanoma— inhibitors of MAP kinase signaling (BRAF inhibitors, vemurafenib and dabrafenib; MEK inhibitors, trametinib and cobimetinib) and large molecule immune checkpoint inhibitors (CTLA-4 inhibitors such as ipilimumab, and PD-1 inhibitors such as nivolumab)—have shown improvements in OS and progression-free survival by a few months in patients with MBM (Falchook et al., 2012; Long et al., 2012; Dummer et al., 2014; Cohen et al., 2016; Margolin, 2016; Spagnolo et al., 2016). Although encouraging (Bates, 2013), it is still difficult to treat advanced

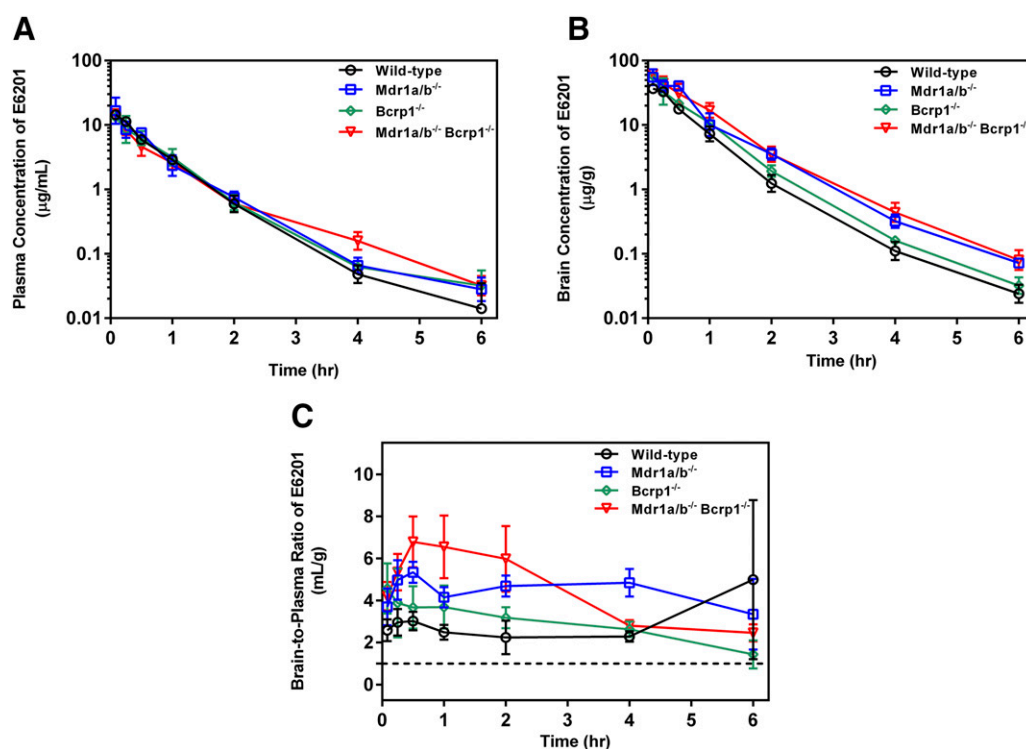


Fig. 3. Pharmacokinetic profiles of E6201 in FVB wild-type, *Mdr1a/b*^{-/-}, *Bcrp1*^{-/-}, and *Mdr1a/b*^{-/-} *Bcrp1*^{-/-} mice following intravenous administration. Plasma concentrations (A), brain concentrations (B), and brain-to-plasma concentration ratios (C) of E6201 in wild-type, *Mdr1a/b*^{-/-}, *Bcrp1*^{-/-}, and *Mdr1a/b*^{-/-} *Bcrp1*^{-/-} mice following administration of single i.v. bolus dose of 40 mg/kg. The dashed line in (C) represents a brain-to-plasma ratio (Kp) of unity. Data represent mean \pm S.D., n = 5.

TABLE 2

The pharmacokinetic/metric parameters of E6201 in FVB wild-type, *Mdr1a/b*^{-/-}, *Bcrp1*^{-/-}, and *Mdr1a/b*^{-/-} *Bcrp1*^{-/-} knockout mice following administration of single i.v. bolus dose of 40 mg/kg

Data are presented as mean or mean ± S.E.M. (n = 5).

	Plasma				Brain			
	Wild-type	<i>Mdr1a/b</i> ^{-/-}	<i>Bcrp1</i> ^{-/-}	<i>Mdr1a/b</i> ^{-/-} <i>Bcrp1</i> ^{-/-}	Wild-Type	<i>Mdr1a/b</i> ^{-/-}	<i>Bcrp1</i> ^{-/-}	<i>Mdr1a/b</i> ^{-/-} <i>Bcrp1</i> ^{-/-}
Half-life (h)	0.65	0.78	0.76	0.83	0.62	0.69	0.60	0.66
AUC _(0-t) (μg·h/ml)	10.20 ± 0.29	10.69 ± 0.75	9.89 ± 0.70	9.36 ± 0.45	27.17 ± 0.95	46.68 ± 2.51	36.78 ± 2.04	50.59 ± 3.09
AUC _(0-∞) (μg·h/ml)	10.21	10.73	9.92	9.40	27.19	46.75	36.81	50.66
CL (ml/min per kilogram)	65.27	62.17	67.17	70.92	—	—	—	—
Vd (l/kg)	3.7	4.2	4.4	5.1	—	—	—	—
Kp (AUC _(0-t) ratio)	-	-	-	-	2.7	4.4	3.7	5.4
Kp _{uu} (AUC _(0-t) ratio)	-	—	—	—	0.14	0.24	0.2	0.29
DA	-	—	—	—	1	1.6	1.4	2

AUC_(0-t), area under the curve from zero to the time of last measured concentration; AUC_(0-∞), area under the curve from zero to time infinity; CL, clearance; DA (distribution advantage), the ratio of Kp_{knockout} to Kp_{wild-type}; Kp (AUC ratio), the ratio of AUC_(0-t,brain) to AUC_(0-t,plasma) using total drug concentrations; Kp_{uu} (AUC ratio), the ratio of AUC_(0-t,brain) to AUC_(0-t,plasma) using free drug concentrations; Vd, volume of distribution.

metastatic disease that has spread to the brain. The modest efficacy in patients with MBM may be related to both inadequate drug delivery and specific brain microenvironment-driven changes in gene expression. Previous studies have shown that vemurafenib, dabrafenib, trametinib, and cobimetinib have limited brain distribution owing to active efflux by Bcrp and/or P-gp (Mittapalli et al., 2012, 2013; Choo et al., 2014; Vaidhyanathan et al., 2014).

E6201, a novel MEK inhibitor, may be beneficial in treatment of melanoma either in combination with a BRAF inhibitor or as a single agent. In the current study, we investigated brain distribution of E6201 in mice, examined the role of efflux transport on brain distribution, and determined its free fraction in plasma and brain. The results help us understand if E6201 can distribute across the BBB to achieve

therapeutically active levels, and also allow us to compare E6201's brain distribution profile with currently available MEK inhibitors. To our knowledge, this is the first report of the brain distribution and active efflux of E6201.

In vitro intracellular accumulation studies in transfected MDCKII cells overexpressing either murine Bcrp or human P-gp strongly suggest that E6201 is not a substrate of Bcrp or P-gp. The intracellular E6201 concentrations were not different between wild-type and Bcrp1/MDR1-transfected cells, and also in Bcrp1- and MDR1-transfected cells treated with and without specific inhibitor of transporter (Fig. 2). Moreover, directional flux studies showed that E6201 was probably not a substrate of P-gp (E6201 investigators brochure). Subsequent experiments tested the influence of Bcrp and/or P-gp on brain distribution of E6201 in vivo.

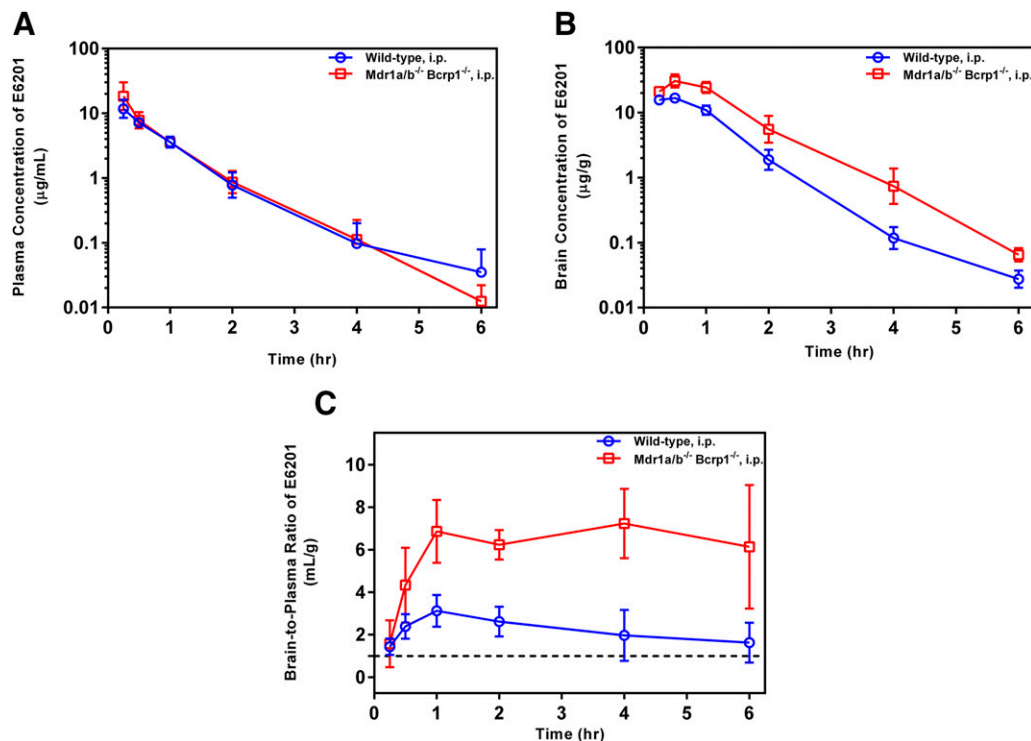


Fig. 4. Pharmacokinetic profiles of E6201 in FVB wild-type and *Mdr1a/b*^{-/-} *Bcrp1*^{-/-} mice following intraperitoneal administration. Plasma concentrations (A), brain concentrations (B), and brain-to-plasma concentration ratios (C) of E6201 in wild-type and *Mdr1a/b*^{-/-} *Bcrp1*^{-/-} mice following administration of single i.p. dose of 40 mg/kg. The dashed line in (C) represents a brain-to-plasma ratio (Kp) of unity. Data represent mean ± S.D., n = 4.

TABLE 3

The pharmacokinetic/metric parameters of E6201 in FVB wild-type and *Mdr1a/b*^{-/-} *Bcrp1*^{-/-} knockout mice following administration of single intraperitoneal dose of 40 mg/kg

Data are presented as mean or mean ± S.E.M. (n = 4).

	Plasma		Brain	
	Wild-type	<i>Mdr1a/b</i> ^{-/-} <i>Bcrp1</i> ^{-/-}	Wild-Type	<i>Mdr1a/b</i> ^{-/-} <i>Bcrp1</i> ^{-/-}
Half-life (h)	0.76	0.62	0.58	0.6
Cmax (μg/ml)	11.70 ± 2.25	18.40 ± 5.80	16.72 ± 1.36	30.75 ± 3.93
Tmax (h)	0.25	0.25	0.5	0.5
AUC _(0-t) (μg*h/ml)	9.69 ± 0.73	11.73 ± 1.57	21.44 ± 1.13	44.93 ± 3.62
AUC _(0-∞) (μg*h/ml)	9.73	11.75	21.46	44.99
CL/F (ml/min per kilogram)	68.5	56.75	—	—
Vd/F (l/kg)	4.5	3.1	—	—
Kp (AUC _(0-t) ratio)	-	-	2.2	3.83
Kp,uu (AUC _(0-t) ratio)	-	—	0.12	0.21
DA	-	—	1	1.75
F	0.95	—	—	—

AUC_(0-t), area under the curve from zero to the time of last measured concentration; AUC_(0-∞), area under the curve from zero to time infinity; CL/F, apparent clearance; Cmax, observed maximum concentration; DA (distribution advantage), the ratio of Kp_{knockout} to Kp_{wild-type}; F (absolute bioavailability), ratio of the dose corrected AUC_(0-t,ip) to dose corrected AUC_(0-t,iv); Kp (AUC ratio), the ratio of AUC_(0-t,brain) to AUC_(0-t,plasma) using total drug concentrations; Kp,uu (AUC ratio), the ratio of AUC_(0-t,brain) to AUC_(0-t,plasma) using free drug concentrations; Tmax, time to reach the maximum concentration; Vd/F, apparent volume of distribution.

In vivo pharmacokinetic experiments following 40 mg/kg single i.v. bolus dose of E6201 indicate that total concentrations in brain were higher than that in plasma at all measured time points in the four genotypes; plasma concentrations were similar (Fig. 3). Consequently, observed AUCs in brain were higher than AUCs in plasma, as can be recognized from the brain-to-plasma AUC ratios (Kp) of 2.66, 4.37, 3.72, and 5.40 in wild-type, *Mdr1a/b*^{-/-}, *Bcrp1*^{-/-}, and *Mdr1a/b*^{-/-} *Bcrp1*^{-/-} mice, respectively (Table 2). Although plasma AUCs were not significantly different, brain AUCs were significantly higher in knockouts compared with wild-type mice. This indicates that P-gp and Bcrp may play a role in limiting E6201's brain delivery; however, the increase in exposure is minimal (2-fold in *Mdr1a/b*^{-/-} *Bcrp1*^{-/-} mice) compared with many substrates reported in literature, for instance cobimetinib [30-fold in *Mdr1a/b*^{-/-} *Bcrp1*^{-/-} mice (Choo et al., 2014)] and trametinib [5-fold in *Mdr1a/b*^{-/-} *Bcrp1*^{-/-} mice (Vaidhyanathan et al., 2014)]. A possibility for the modest increase in Kp (≤2-fold), given the in vitro results, could be related to changes in transporter expression in knockout mice. Though a change in expression could be possible for some unknown transporter, it is improbable here, given that the results of transporter, receptor, and tight junction proteomic analysis in wild-type compared with *Mdr1a/b*^{-/-} and/or *Bcrp1*^{-/-} mice (Agarwal et al., 2012) indicated no change in expression of BBB proteins. Nevertheless, these results show that E6201, for a molecularly

targeted agent, has brain distribution characteristics that are minimally influenced by Bcrp and P-gp efflux at the BBB.

The brain partitioning following intraperitoneal and oral administration of E6201 at the same dose was similar to that observed in intravenous studies. The absolute bioavailability (F) of E6201 was higher following intraperitoneal dosing compared with oral dosing (F = 0.95, i.p., F = 0.39, by mouth; Tables 3 and 4). Consistent with in vitro results, in vivo studies characterizing the brain exposure of E6201 demonstrate that neither Bcrp nor P-gp show a marked involvement in limiting the brain delivery of E6201.

In vitro rapid equilibrium dialysis experiments indicate that E6201 exhibits higher nonspecific binding in brain compared with plasma, possibly related to lipophilic brain environment, with free fractions (fu) of 0.14% and 2.63%, respectively (Table 1). The fu values were used to estimate the unbound partition coefficients (Kp,uu) in wild-type, *Mdr1a/b*^{-/-}, *Bcrp1*^{-/-}, and *Mdr1a/b*^{-/-} *Bcrp1*^{-/-} mice, 0.14, 0.24, 0.2, and 0.29, respectively, following intravenous dosing (Table 2). The Kp,uu values in all four genotypes of mice were less than one, indicating a distribution disequilibrium (Di et al., 2013; Summerfield et al., 2016). It is probable that E6201 has a high passive permeability in the absence of active efflux, since it is a relatively small molecule (389.45 g/mol), highly lipophilic [xlogP3 = 3.3 (PubChem), logP = 3.63 (E6201 investigators brochure)], and not significantly charged at physiologic

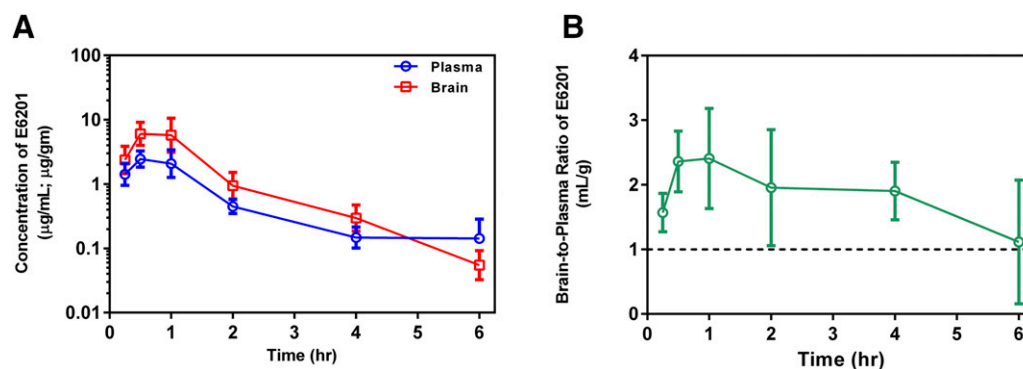


Fig. 5. Pharmacokinetic profiles of E6201 in FVB wild-type mice following oral administration. Plasma concentrations and brain concentrations (A), and brain-to-plasma concentration ratios (B) of E6201 in wild-type mice upon single dose PO of 40 mg/kg. The dashed line in (B) represents a brain-to-plasma ratio (Kp) of unity. Data represent mean ± S.D., n = 4.

TABLE 4

E6201 pharmacokinetic/metric parameters in FVB wild-type mice following administration of single oral dose of 40 mg/kg

Data are presented as mean or mean \pm S.E.M. (n = 4).

	Plasma	Brain
Half-life (h)	1.37	0.98
C _{max} (μ g/ml)	2.44 \pm 0.41	6.04 \pm 1.55
T _{max} (h)	0.5	0.5
AUC _(0-t) (μ g*h/ml)	3.94 \pm 0.54	9.23 \pm 1.95
AUC _(0-∞) (μ g*h/ml)	4.22	9.31
CL/F (ml/min per kilogram)	158	—
Vd/F (l/kg)	18.7	—
K _p (AUC _(0-t) ratio)	-	2.35
K _{p,uu} (AUC _(0-t) ratio)	-	0.13
F	0.39	—

AUC_(0-t), area under the curve from zero to the time of last measured concentration; AUC_(0-∞), area under the curve from zero to time infinity; CL/F, apparent clearance; C_{max}, observed maximum concentration; F (absolute bioavailability), ratio of the dose corrected AUC_(0-t,PO) to dose corrected AUC_(0-t,iv); K_p (AUC ratio), the ratio of AUC_(0-t,brain) to AUC_(0-t,plasma) using total drug concentrations; K_{p,uu} (AUC ratio), the ratio of AUC_(0-t,brain) to AUC_(0-t,plasma) using free drug concentrations; PO, by mouth; T_{max}, time to reach the maximum concentration; Vd/F, apparent volume of distribution.

pH [pKa of basic nitrogen = 8.8 (E6201 investigators brochure)]. Also, it can be seen from the brain-to-plasma ratio plot for the four genotypes (Fig. 3C) that an equilibrium between brain and plasma concentrations is achieved rapidly (\sim 0.5 hour) suggesting a high rate into brain. Given these observations, it is possible that K_{p,uu} less than unity is related to efflux transporter(s) other than Bcrp and P-gp that are influencing E6201's brain delivery, especially given that K_{p,uu} in *Mdr1a/b*^{-/-} *Bcrp1*^{-/-} mice is also less than unity.

The average free-drug concentrations in wild-type mice were determined at measured time points to obtain the free concentration-time profile. The free concentrations were then compared with in vitro potency estimates in melanoma cell lines to evaluate the potential of E6201 for treatment of MBM. The free concentrations in brain reached levels higher than the reported IC₅₀ value (IC₅₀ = 43.7 nmol/l, SK-MEL-28 melanoma cell line; E6201 investigators brochure), suggesting that E6201 may show efficacy in treatment of MEK-driven brain tumors (Fig. 6). Also, since the IC₅₀ measurements employed total and not free concentrations in media, the free IC₅₀ can be expected to be even lower, giving further credence to the idea that adequate delivery may be achieved in vivo. Given such insights, it would be valuable to conduct efficacy studies with E6201 in preclinical models of MBM as a next step to better understand in vivo efficacy, leading to clinical trials.

The unique macrocyclic structure of E6201 may enhance its brain penetration by avoiding active efflux via Bcrp and P-gp. A macrocyclic structure facilitates a reduction in rotatable bonds, reported to positively correlate with improved brain penetration by lessening active efflux (Heffron, 2016). Also, of at least equal, and probably greater, significance is the opportunity for formation of intramolecular hydrogen bonds that can effectively mask hydrogen-bond donors (HBD), which have a profound correlation with the probability of transporter-mediated efflux (Heffron, 2016). The three-dimensional X-ray crystal structure of E6201 bound to MEK (see <http://www.rcsb.org/pdb/explore.do?structureId=5HZE>) shows that each of the alcohol/phenol "OH" groups are capable of intramolecular hydrogen bonding, thereby allowing effective masking of three of the four available HBDs, essentially leaving only one effective HBD. Such observations have been reported for other targeted agents such as lorlatinib [anaplastic lymphoma kinase (ALK) inhibitor] and AZD3759 [epidermal growth factor receptor (EGFR) inhibitor] (Johnson et al., 2014; Zeng et al., 2015). Recent literature highlights the fact that an optimal balance of physicochemical properties is necessary to achieve adequate distribution

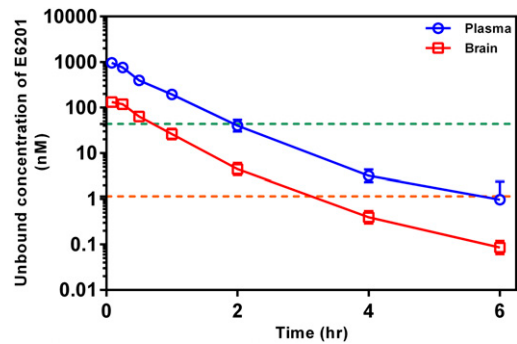


Fig. 6. Plasma and brain unbound concentration-time profile of E6201 in FVB wild-type mice. The dashed green line represents the reported in vitro E6201 IC₅₀ against SK-MEL-28 melanoma cell line (IC₅₀ = 43.7 nmol/l, E6201 investigator brochure). The dashed orange line represents the free E6201 IC₅₀ determined using the plasma free fraction of E6201 ($f_{u,plasma}$ = 0.026, free IC₅₀ = 1.14 nmol/l). Here, the assumption is that the nonspecific binding of E6201 in the assay media is similar to the free fraction determined in plasma experimentally. Data represent mean \pm S.D., n = 5.

to brain, and drugs having low molecular weight, fewer rotatable bonds, low total polar surface area, and fewer HBDs are expected to have better CNS penetration (Rankovic, 2015; Heffron, 2016; Wager et al., 2016). The combination of few rotatable bonds and few effective HBDs readily explains how E6201 achieves significant brain distribution.

In the context of brain tumors, it is important to note that the approved MEK inhibitors trametinib and cobimetinib show limited brain distribution owing to active efflux. The K_p for trametinib and cobimetinib in wild-type mice were 0.15 and 0.32, respectively (Table 5). As evident from the K_p of 2.66 in wild-type mice, the total concentrations for E6201 are higher in brain compared with plasma, unlike for trametinib and cobimetinib. Given that the three MEK inhibitors are highly protein-bound, K_{p,uu} for E6201 is much higher than that of cobimetinib and similar to that of trametinib (Table 5). The brain distribution profile of E6201 makes it an attractive MEK inhibitor for the treatment of MBM, with potential for achieving improved treatment responses.

The development of targeted agents inhibiting the MAPK pathway and immunotherapies has led to major advances in the treatment of patients with metastatic melanoma. However, it is crucial to recognize the challenges that still remain in delivering the molecularly targeted agents to tumor cells in the brain that may be growing behind an intact BBB. Both the brain microenvironment-driven changes in genetic expression leading to resistance and CNS drug-delivery issues need to be addressed to achieve a clinically meaningful response in MBM and other brain tumors. Though single-agent treatment may show responses, there is a need to test rational combinations (e.g., a BRAF inhibitor and MEK inhibitor to better inhibit MAPK pathway; a BRAF/MEK inhibitor and a

TABLE 5

Comparison of brain distribution of MEK inhibitors in wild-type mice

Data are presented as means.

MEK Inhibitor	Dose	K _p	$f_{u,brain}$	$f_{u,plasma}$	K _{p,uu}
	mg/kg				
Trametinib	5 (i.v.)	0.15 ^a	0.0021	0.0021	0.15
Cobimetinib ^b	10 (PO)	0.32	0.0012	0.014	0.027
E6201	40 (i.v.)	2.66	0.0014	0.034	0.14

f_u , free (unbound) fraction; K_p (AUC ratio), the ratio of AUC_(0-t,brain) to AUC_(0-t,plasma) using total drug concentrations; K_{p,uu} (AUC ratio), the ratio of AUC_(0-t,brain) to AUC_(0-t,plasma) using free drug concentrations; PO, by mouth.

^aK_p reported by Vaidhyanathan et al. (2014).

^bResults reported by Choo et al. (2014); K_p and K_{p,uu} on the basis of plasma and brain concentrations 6 hours postdose.

PI3K/mTOR inhibitor to inhibit both MAPK and PI3K pathways) in order to tackle issues of resistance to therapy. When using combinations, it is important to examine CNS distribution of all agents in the combination regimen since all administered drugs should adequately reach the target site in brain to achieve desired responses and minimize emergence of resistance. Despite the remarkable progress, there remains a need to develop better therapies for MBMs, and drug delivery across the BBB is one crucial factor that requires attention to fulfill this goal.

Acknowledgments

The authors thank Jim Fisher, Clinical Pharmacology Analytical Laboratory, University of Minnesota, for his support in the development of the LC-MS/MS assays, and Timothy Heffron from Genentech Inc. for his valuable input.

Authorship Contributions

Participated in research design: Gampa, Kim, Laramy, Sarkaria, Paradiso, DePalatis, Elmquist.

Conducted experiments: Gampa, Kim, Cook-Rostie, Laramy.

Performed data analysis: Gampa, Kim, Laramy, Elmquist.

Wrote or contributed to the writing of the manuscript: Gampa, Laramy, Sarkaria, Paradiso, DePalatis, Elmquist.

References

- Agarwal S, Sane R, Oberoi R, Ohlfest JR, and Elmquist WF (2011) Delivery of molecularly targeted therapy to malignant glioma, a disease of the whole brain. *Expert Rev Mol Med* 13:e17.
- Agarwal S, Uchida Y, Mittapalli RK, Sane R, Terasaki T, and Elmquist WF (2012) Quantitative proteomics of transporter expression in brain capillary endothelial cells isolated from P-glycoprotein (P-gp), breast cancer resistance protein (Bcrp), and P-gp/Bcrp knockout mice. *Drug Metab Dispos* 40:1164–1169.
- Bates SE (2013) A sea change in melanoma. *Clin Cancer Res* 19:5282.
- Byron SA, Loch DC, Wellens CL, Wortmann A, Wu J, Wang J, Nomoto K, and Pollock PM (2012) Sensitivity to the MEK inhibitor E6201 in melanoma cells is associated with mutant BRAF and wildtype PTEN status. *Mol Cancer* 11:75.
- Choo EF, Ly J, Chan J, Shahidi-Latham SK, Messick K, Plise E, Quiason CM, and Yang L (2014) Role of P-glycoprotein on the brain penetration and brain pharmacodynamic activity of the MEK inhibitor cobimetinib. *Mol Pharm* 11:4199–4207.
- Cohen JV, Tawbi H, Margolin KA, Amravadi R, Bosenberg M, Brastianos PK, Chiang VL, de Groot J, Glitza IC, Herlyn M, et al. (2016) Melanoma central nervous system metastases: current approaches, challenges, and opportunities. *Pigment Cell Melanoma Res* 29:627–642.
- Dai H, Marbach P, Lemaire M, Hayes M, and Elmquist WF (2003) Distribution of STI-571 to the brain is limited by P-glycoprotein-mediated efflux. *J Pharmacol Exp Ther* 304:1085–1092.
- Damsky WE, Theodosakis N, and Bosenberg M (2014) Melanoma metastasis: new concepts and evolving paradigms. *Oncogene* 33:2413–2422.
- Davies H, Bignell GR, Cox C, Stephens S, Clegg S, Teague J, Woffendin H, Garnett MJ, Bottomley W, et al. (2002) Mutations of the BRAF gene in human cancer. *Nature* 417:949–954.
- Di L, Rong H, and Feng B (2013) Demystifying brain penetration in central nervous system drug discovery. *Miniperspective. J Med Chem* 56:2–12.
- Dummer R, Goldinger SM, Turtzsch CP, Eggmann NB, Michielin O, Mitchell L, Veronese L, Hilfiker PR, Felderer L, and Rinderknecht JD (2014) Vemurafenib in patients with BRAF(V600) mutation-positive melanoma with symptomatic brain metastases: final results of an open-label pilot study. *Eur J Cancer* 50:611–621.
- Essig M, Weber M-A, von Tengg-Kobligh K, Knopp MV, Yuh WTC, and Giesel FL (2006) Contrast-enhanced magnetic resonance imaging of central nervous system tumors: agents, mechanisms, and applications. *Top Magn Reson Imaging* 17:89–106.
- Falchook GS, Long GV, Kurzrock R, Kim KB, Arkenau TH, Brown MP, Hamid O, Infante JR, Millward M, Pavlick AC, et al. (2012) Dabrafenib in patients with melanoma, untreated brain metastases, and other solid tumours: a phase 1 dose-escalation trial. *Lancet* 379:1893–1901.
- Fife KM, Colman MH, Stevens GN, Firth IC, Moon D, Shannon KF, Harman R, Petersen-Schaefer K, Zacest AC, Besser M, et al. (2004) Determinants of outcome in melanoma patients with cerebral metastases. *J Clin Oncol* 22:1293–1300.
- Flaherty KT, Infante JR, Daud A, Gonzalez R, Kefford RF, Sosman J, Hamid O, Schuchter L, Cebon J, Ibrahim N, et al. (2012) Combined BRAF and MEK inhibition in melanoma with BRAF V600 mutations. *N Engl J Med* 367:1694–1703.
- Fridén M, Gupta A, Antonsson M, Bredberg U, and Hammarlund-Udenaes M (2007) In vitro methods for estimating unbound drug concentrations in the brain interstitial and intracellular fluids. *Drug Metab Dispos* 35:1711–1719.
- Gampa G, Vaidhyanathan S, Resman BW, Parrish KE, Markovic SN, Sarkaria JN, and Elmquist WF (2016) Challenges in the delivery of therapies to melanoma brain metastases. *Curr Pharmacol Rep* 2:309–325.
- Gampa G, Vaidhyanathan S, Sarkaria JN, and Elmquist WF (2017) Drug delivery to melanoma brain metastases: can current challenges lead to new opportunities? *Pharmacol Res* 123:10–25.
- Goto M, Chow J, Muramoto K, Chiba K, Yamamoto S, Fujita M, Obaishi H, Tai K, Mizui Y, Tanaka I, et al. (2009) E6201 [(3S,4R,5S,8S,9S,11E)-14-(ethylamino)-8, 9,16-trihydroxy-3,4-dimethyl-3,4,9,19-tetrahydro-1H-2-benzoxacyclotetradecine-1,7(8H)-dione], a novel kinase inhibitor of mitogen-activated protein kinase/extracellular signal-regulated kinase kinase (MEK)-1 and MEK kinase-1: in vitro characterization of its anti-inflammatory and antihyperproliferative activities. *J Pharmacol Exp Ther* 331:485–495.
- Gupta G, Robertson AG, and MacKie RM (1997) Cerebral metastases of cutaneous melanoma. *Br J Cancer* 76:256–259.
- Heffron TP (2016) Small molecule kinase inhibitors for the treatment of brain cancer. *J Med Chem* 59:10030–10066.
- Hocker T and Tsao H (2007) Ultraviolet radiation and melanoma: a systematic review and analysis of reported sequence variants. *Hum Mutat* 28:578–588.
- Ikemori-Kawada M, Inoue A, Goto M, Wang YJ, and Kawakami Y (2012) Docking simulation study and kinase selectivity of f152A1 and its analogs. *J Chem Inf Model* 52:2059–2068.
- Johnson TW, Richardson PF, Bailey S, Brooun A, Burke BJ, Collins MR, Cui JJ, Deal JG, Deng YL, Dinh D, et al. (2014) Discovery of (10R)-7-amino-12-fluoro-2,10,16-trimethyl-15-oxo-10,15,16,17-tetrahydro-2H-8,4-(metheno)pyrazolo[4,3-h][2,5,11]-benzoxadiazacyclotetradecine-3-carbonitrile (PF-06463922), a macrocyclic inhibitor of anaplastic lymphoma kinase (ALK) and c-ros oncogene 1 (ROS1) with preclinical brain exposure and broad-spectrum potency against ALK-resistant mutations. *J Med Chem* 57:4720–4744.
- Kalvass JC and Maurer TS (2002) Influence of nonspecific brain and plasma binding on CNS exposure: implications for rational drug discovery. *Biopharm Drug Dispos* 23:327–338.
- Larkin J, Ascierto PA, Dréno B, Atkinson V, Liszkay G, Maio M, Mandalà M, Demidov L, Stroyakovskiy D, Thomas L, et al. (2014) Combined vemurafenib and cobimetinib in BRAF-mutated melanoma. *N Engl J Med* 371:1867–1876.
- Lito P, Rosen N, and Solit DB (2013) Tumor adaptation and resistance to RAF inhibitors. *Nat Med* 19:1401–1409.
- Long GV, Trefzer U, Davies MA, Kefford RF, Ascierto PA, Chapman PB, Puzanov I, Hauschild A, Robert C, Algazi A, et al. (2012) Dabrafenib in patients with Val600Glu or Val600Lys BRAF-mutant melanoma metastatic to the brain (BREAK-MB): a multicentre, open-label, phase 2 trial. *Lancet Oncol* 13:1087–1095.
- Margolin K (2016) The promise of molecularly targeted and immunotherapy for advanced melanoma. *Curr Treat Options Oncol* 17:48.
- Mittapalli RK, Vaidhyanathan S, Dudek AZ, and Elmquist WF (2013) Mechanisms limiting distribution of the threonine-protein kinase B-Raf(V600E) inhibitor dabrafenib to the brain: implications for the treatment of melanoma brain metastases. *J Pharmacol Exp Ther* 344:655–664.
- Mittapalli RK, Vaidhyanathan S, Sane R, and Elmquist WF (2012) Impact of P-glycoprotein (ABCB1) and breast cancer resistance protein (ABCG2) on the brain distribution of a novel BRAF inhibitor: vemurafenib (PLX4032). *J Pharmacol Exp Ther* 342:33–40.
- Murrell DH, Hamilton AM, Mallett CL, van Gorkum R, Chambers AF, and Foster PJ (2015) Understanding heterogeneity and permeability of brain metastases in murine models of HER2-positive breast cancer through magnetic resonance imaging: implications for detection and therapy. *Transl Oncol* 8:176–184.
- Narita Y, Okamoto K, Kawada MI, Takase K, Minoshima Y, Kodama K, Iwata M, Miyamoto N, and Sawada K (2014) Novel ATP-competitive MEK inhibitor E6201 is effective against vemurafenib-resistant melanoma harboring the MEK1-C121S mutation in a preclinical model. *Mol Cancer Ther* 13:823–832.
- Nedelman JR and Jia X (1998) An extension of Satterthwaite's approximation applied to pharmacokinetics. *J Biopharm Stat* 8:317–328.
- Osswald M, Blaes J, Liao Y, Solecki G, Gömmel M, Berghoff AS, Salphati L, Wallin JJ, Phillips HS, Wick W, et al. (2016) Impact of blood-brain barrier integrity on tumor growth and therapy response in brain metastases. *Clin Cancer Res* 22:6078–6087.
- Raizer JJ, Hwu W-J, Panageas KS, Wilton A, Baldwin DE, Bailey E, von Althann C, Lamb LA, Alvarado G, Bilsky MH, et al. (2008) Brain and leptomeningeal metastases from cutaneous melanoma: survival outcomes based on clinical features. *Neuro-oncol* 10:199–207.
- Rankovic Z (2015) CNS drug design: balancing physicochemical properties for optimal brain exposure. *J Med Chem* 58:2584–2608.
- Ribas A, Gonzalez R, Pavlick A, Hamid O, Gajewski TF, Daud A, Flaherty L, Logan T, Chmielowski B, Lewis K, et al. (2014) Combination of vemurafenib and cobimetinib in patients with advanced BRAF(V600)-mutated melanoma: a phase 1b study. *Lancet Oncol* 15:954–965.
- Samatar AA and Poulikakos PI (2014) Targeting RAS-ERK signalling in cancer: promises and challenges. *Nat Rev Drug Discov* 13:928–942.
- Siegel RL, Miller KD, and Jemal A (2017) Cancer statistics, 2017. *CA Cancer J Clin* 67:7–30.
- Sloan AE, Nock CJ, and Einstein DB (2009) Diagnosis and treatment of melanoma brain metastasis: a literature review. *Cancer Contr* 16:248–255.
- Spagnolo F, Picasso V, Lamberti M, Ottaviano V, Dozin B, and Queirolo P (2016) Survival of patients with metastatic melanoma and brain metastases in the era of MAP-kinase inhibitors and immunologic checkpoint blockade antibodies: a systematic review. *Cancer Treat Rev* 45:38–45.
- Summerfield SG, Zhang Y, and Liu H (2016) Examining the uptake of central nervous system drugs and candidates across the blood-brain barrier. *J Pharmacol Exp Ther* 358:294–305.
- Vaidhyanathan S, Mittapalli RK, Sarkaria JN, and Elmquist WF (2014) Factors influencing the CNS distribution of a novel MEK-1/2 inhibitor: implications for combination therapy for melanoma brain metastases. *Drug Metab Dispos* 42:1292–1300.
- Wager TT, Hou X, Verhoest PR, and Villalobos A (2016) Central nervous system multiparameter optimization desirability: application in drug discovery. *ACS Chem Neurosci* 7:767–775.
- Zeng Q, Wang J, Cheng Z, Chen K, Johnström P, Vamias K, Li DY, Yang ZF, and Zhang X (2015) Discovery and evaluation of clinical candidate AZD3759, a potent, oral active, central nervous system-penetrant, epidermal growth factor receptor tyrosine kinase inhibitor. *J Med Chem* 58:8200–8215.

Address correspondence to: Dr. William F. Elmquist, Department of Pharmaceuticals, University of Minnesota, 308 Harvard Street SE, Minneapolis, MN 55455. E-mail: elmqu011@umn.edu